

# Raman, FT-IR and XRD investigation of natural opals

A. Sodo,<sup>a\*</sup> A. Casanova Municchia,<sup>a</sup> S. Barucca,<sup>a</sup> F. Bellatreccia,<sup>a</sup>  
G. Della Ventura,<sup>a</sup> F. Butini<sup>b</sup> and M. A. Ricci<sup>a</sup>



Opals are naturally occurring hydrous silica materials ( $\text{SiO}_2 \cdot n\text{H}_2\text{O}$ ), characterized by different degrees of crystallinity and crystal structure. Because of their optical properties, opals have been largely used in jewelry and as decorative elements in artworks. For this reason, a complete characterization and a provenance study of this kind of materials is mandatory in order both to avoid frauds and to reconstruct ancient and modern trade routes of gems. In this work, we present a combined spectroscopic (Raman, FTIR) and X-ray powder diffraction (XRD) investigation of nine opals from the main deposits around the world (Australia, Madagascar, Slovakia, Mexico, Honduras and Ethiopia). Four of these samples are the rare and precious fire opals, characterized by an intense red–orange color. Ethiopia, Honduras and Mexico opals showed spectra and diffraction patterns typical of Opal-CT, generally associated to volcanic genesis, while Australia, Madagascar and Slovakia opals are Opal-A type, associated to sedimentary origin. Unexpectedly the fire opal from Brazil behaves as a CT one. The presence of  $\text{CO}_2$  was detected only in the latter group, and exceptionally in the Honduras sample; FTIR-FPA imaging showed carbon dioxide to be homogeneously distributed inside the gems. Opals-CT are  $\text{CO}_2$ -free and give much more complex FT-IR spectra in the NIR region where  $\text{H}_2\text{O}$  combination modes occur. The obtained results are discussed in terms of relevance of the above experimental techniques for geosourcing opals, and contribute to increase the database of the chemical–physical properties of opals. Copyright © 2016 John Wiley & Sons, Ltd.

Additional supporting information may be found in the online version of this article at the publisher's web site.

**Keywords:** opals; Raman; XRD; FT-IR

## Introduction

Opals are water-bearing micro- to non-crystalline materials, composed of micro-spheres of hydrated silica ( $\text{SiO}_2 \cdot n\text{H}_2\text{O}$ ) with a high degree of structural disorder.<sup>[1,2]</sup> Because of their optical properties, opals have been largely used in jewelry and as decorative elements in art works.<sup>[3]</sup> Because of the high economic value, rarity and preciousness of natural opals, different kind of imitations and synthetic opals are available on the market and have sometimes replaced original gems in artworks.

The characteristic optical phenomenon of the opal, called 'play of color', is because of the interaction of light with their pseudo-structure composed of regularly spaced layers consisting of sub-micron sized (average diameter few hundreds of nm) silica spheres.<sup>[4–8]</sup> The presence or absence of this optical phenomenon determines the gemological classification: 'play of colour' opals, sometimes called noble opals, show this effect, whereas common opals do not. Nevertheless, also some common opals are attractive because of their usually opaque to translucent body colour. Although some rare opals are colorless, most specimens present a body colour: white, black, gray, brown, yellow to orange (as in fire opal), red, pink, blue, green or violet, depending on mineral inclusions and on the presence of particular trace elements.<sup>[9–15]</sup> A number of these common opals have also a significant commercial value, as for instance the pink opals from Acari (Peru).

Opals differ in the crystallinity degree and in crystal-structure arrangement. Based on the mineralogical composition,<sup>[16]</sup> opals can be classified into three typologies, depending on the main constituent revealed by X-rays diffraction (XRD). Opal-C is a well-ordered form,

consisting predominantly of  $\alpha$ -cristobalite; opal-CT is semi-crystalline and consists of crystalline regions of  $\alpha$ -cristobalite and  $\alpha$ -tridymite; finally opal-A, the most disordered typology, is predominantly amorphous and corresponds to the most disordered structure.

More recently, two further different classifications have been proposed: the first is based on Raman spectroscopy, which clearly distinguish between opals-A and opals-CT.<sup>[17,18]</sup> According to this classification, opals-CT, generally of volcanic origin, are more crystalline than opals-A, generally of sedimentary origin. The second classification, proposed by Rondeau *et al.* in their work on opals from Slovakia,<sup>[19]</sup> groups opals according to their formation temperature. The 'low temperature' type includes opals previously characterized as sedimentary (formed at  $T < 45^\circ\text{C}$ ), while the 'high temperature' group includes the volcanic ones (formed at  $100^\circ\text{C} < T < 170^\circ\text{C}$ ).

In literature, there are few studies of common opals of gemological interest, with the exception of Australian 'potch' opal which have attracted more interest.<sup>[20,21]</sup> On the contrary, it is possible to find extensive studies of common opals of geological significance.<sup>[6,22–31]</sup> In most of these studies, the classical mineralogical and the Raman classification are used.

Aim of this work is the characterization of nine natural opals from the main known deposits all around the world: Australia, Brazil,

\* Correspondence to: Armida Sodo, Università Roma Tre, Dipartimento di Scienze, Viale G. Marconi 446, Italy. E-mail: sodo@fis.uniroma3.it

a Università Roma Tre, Dipartimento di Scienze, Viale G. Marconi 446, 00146, Rome, Italy

b IGN, Istituto Gemmologico Nazionale, Via S. Sebastianello 6, 00187, Rome, Italy

Ethiopia, Honduras, Madagascar, Mexico and Slovakia. The samples have been studied with the aim of defining a method to assess their geological provenance.

As it is well discussed in the work of Gaillou *et al.* (2008),<sup>[12]</sup> the identification of the chemical and physical properties of opals from a particular geographic area is important for several reasons. For instance, in the gem market, stones coming from specific localities can be more valuable than others. In addition, in the archaeometrical investigation, knowledge of the geographic origin is crucial to reconstruct the ancient trade routes of gems.<sup>[12,32]</sup> In historical times opals came almost exclusively from the deposits of Cernowitz, in the actual Slovakia. Later, other deposits were discovered in various locations around the world; at present, almost all of the opals on the market originate from Australia.

Because of the structural disorder at long range, hydrous silica is a rather complex material, and its study requires the combination of different analytical methods. In this work, we combine information obtained by Raman spectroscopy, FTIR absorbance and XRD investigations.

Raman spectroscopy is a suitable tool to investigate opals<sup>[17,18,33,34]</sup> and to identify their different geological provenance, because of its ability to detect the presence of nano-sized domains of silica polymorphs, as well as the presence of non-crystalline phases in the assemblage. The spectroscopic data have been implemented by X-rays powder diffraction (XRD) for long-range order information and FTIR for detecting the possible presence and distribution of H<sub>2</sub>O/OH, CO<sub>2</sub> and other molecular arrangements for a complete characterization of the material.<sup>[9,12,15]</sup>

## Experimental

### Samples

Nine natural opals from the main deposits around the world (Australia, Brazil, Ethiopia, Honduras, Madagascar, Mexico and Slovakia) have been investigated by Raman, FT-IR spectroscopies and XRD diffraction. Their colors range from white, yellowish white, orange, orange–red (fire opals), reddish orange to brown. Four of them are fire opals and are labeled with ‘-FO’ in this work. Most of them are rough and only one of them is cut in cabochon (Ethiopia). They present a luster from greasy to vitreous and their degree of transparency varies from translucent to opaque. Only one opal from Ethiopia can be defined as noble showing an intense play of colors. All the other samples are common opals, not showing any appreciable play of colors. In Table 1, we report all the information for each investigated sample and in Fig. 1 we show the sample photographs taken at the stereo-microscope.

### Raman spectroscopy

All opals were preliminary investigated using a Renishaw In-Via Reflex Raman microscope equipped with three different sources, at 785.5, 633 and 514.5 nm respectively, in order to choose the best experimental conditions. The final spectra have been collected by using the 633-nm He–Ne laser, with a nominal output power set at 18 mW. Neutral filters were not used to reduce laser power on the samples because no degradation was observed. The illumination and collecting optics of the system consisted of a confocal microscope configuration. The system achieves the high contrast required for the rejection of the elastically scattered component by an edge filter. The backscattered light is dispersed by a 1800 line/mm grating and the Raman signal is detected by a Peltier

**Table 1.** list of investigated samples and their gemmological information

Samples	Origin	Description	Color	Transparency	Luster	Play of color	Provenance	Archive number
Australia	Australia	Rough	White	Translucent	Vitreous to greasy	No	Museum National d'Histoire Naturelle, Paris	JMF1
Brazil-FO	Brazil	Rough	Orange–red (fire opal)	Translucent	Vitreous to greasy	No	Museum National d'Histoire Naturelle, Paris	OP656
Ethiopia	Ethiopia	Cabochon	Brown	Opaque	Vitreous	Yes	Private collection	—
Ethiopia-FO	Ethiopia	Rough	Orange–red (fire opal)	Translucent	Vitreous to greasy	No	Museum National d'Histoire Naturelle, Paris	OP2
Honduras	Honduras	Rough	Yellowish-white	Translucent	Vitreous to greasy	No	Museum National d'Histoire Naturelle, Paris	OP639
Madagascar	Madagascar	Rough	White	Translucent	Vitreous to greasy	No	Museum National d'Histoire Naturelle, Paris	114.60a
Mexico-FO1	Mexico	Pebbles/rough	Orange–red (fire opal)	Translucent	Vitreous to greasy	No	Private collection	—
Mexico-FO2	Mexico	Rough	Orange–red (fire opal)	Translucent	Vitreous to greasy	No	Museum National d'Histoire Naturelle, Paris	OF3
Slovakia	Slovakia	Rough	White	Translucent	Vitreous to greasy	No	Museum National d'Histoire Naturelle, Paris	MINH1



**Figure 1.** Photographs taken at the stereo-microscope of the investigated samples. The black bar corresponds to 5 mm.

cooled ( $-70^{\circ}\text{C}$ )  $1024 \times 256$  pixel CCD detector. Nominal spectral resolution is about  $1\text{ cm}^{-1}$ . For each sample, we performed three measurements on different points. Spectral acquisitions (3 accumulations, 20 s each, in the range  $100\text{--}3400\text{ cm}^{-1}$ ) have been performed with  $20\times$  objectives. Origin 8 software was used for the spectra elaboration (baseline correction to remove background fluorescence when necessary).

### FT-IR spectroscopy

Powder FTIR spectra were collected at Università Roma Tre, on a Nicolet iS50 FTIR spectrometer equipped with a DTGS detector and a KBr beamsplitter; approximately 2 mg of sample was mixed in 200 mg of KBr; spectra were collected in the range  $400\text{--}4000\text{ cm}^{-1}$ , averaging 64 scans for both sample and background and with a  $4\text{ cm}^{-1}$  nominal resolution. Micro-FTIR spectra and FTIR images were collected at the Laboratori Nazionali di Frascati-Istituto Nazionale di Fisica Nucleare (LNF-INFN), Frascati (Rome), with a Bruker® Hyperion 3000 IR microscope equipped with a MCT-A nitrogen-cooled detector; FTIR images were collected using a  $64 \times 64$ -pixel focal-plane array (FPA) of liquid nitrogen-cooled MCT detectors. Single-spot spectra were collected using a beam size varying from 50 to  $100\text{ }\mu\text{m}$ , in the range  $650\text{--}7000\text{ cm}^{-1}$ , averaging 128 scans for both sample and background and with a  $4\text{ cm}^{-1}$  nominal resolution. FTIR images were acquired with a nominal resolution set at  $4\text{ cm}^{-1}$  and 64 scans were averaged for each spectrum and background. Images, collected using a  $15\times$  objective, cover an area of  $170 \times 170\text{ }\mu\text{m}^2$  with a nominal spatial resolution of  $\sim 5\text{ }\mu\text{m}$ .<sup>[35]</sup>

### X-ray powder diffraction (XRD)

The powder X-ray diffraction data were collected at Dipartimento di Scienze, Università Roma Tre, with a Scintag X1 diffractometer using  $\text{CuK}\alpha_1$  radiation ( $\lambda = 1.54055\text{ \AA}$ , 40 mA, 45 kV), fixed divergent slits and a Peltier-cooled Si(Li) detector (resolution  $< 200\text{ eV}$ ). A divergent slit width of 2 mm and a scatter slit width of 4 mm were employed for the beam source; a receiving slit width of 0.5 mm and scatter slit width of 0.2 mm were used for the detector. Data were collected in step-scan mode:  $15\text{--}70^{\circ}$   $2\theta$  range, step-size  $0.05^{\circ}$   $2\theta$ , counting time 15 s/step.

The samples for micro-FTIR were prepared as double-polished slabs to thickness variable from 80 to  $260\text{ }\mu\text{m}$ ; the samples thickness was measured with a digital micrometer.

## Results and discussion

### Raman measurements

Before performing Raman measurements, opals have been observed under an optical microscope by using 20, 50 and  $100\times$  objectives, in order to investigate the homogeneity of the samples. At this level, no inhomogeneities have been observed. For the same reason, three different points for each sample have been selected to collect Raman spectra and a long distance  $20\times$  objective has been chosen to average a larger area. For each sample, all three Raman spectra collected perfectly overlap, thus confirming the homogeneity of the investigated samples.

In this work, Raman spectroscopy has been used to investigate the degree of crystallinity of the opals; for this reason, spectra have been shown in the range  $200\text{--}1100\text{ cm}^{-1}$ . To check for the presence and distribution of  $\text{H}_2\text{O/OH}$  and  $\text{CO}_2$ , micro FT-IR measurements have been performed because of the highest sensibility of this technique, compared to Raman to detect water and carbon dioxide.

Generally, opals exhibit strong Raman signals in the range  $200\text{--}600\text{ cm}^{-1}$ , which is typical of framework silicates (Si—O—Si bending). In all the opal spectra, these bands are very broad, indicating that also the more crystalline samples are significantly amorphous. According to literature,<sup>[18]</sup> the position of the apparent maximum of the most intense band in this range can be used to distinguish opals-CT, showing a maximum around  $335\text{ cm}^{-1}$ , from opals-A that are characterized by a broad band with maximum at  $430\text{ cm}^{-1}$ . This difference in band position has been observed and well reported for opals-A from Brazil and Australia<sup>[17,36]</sup> and for Slovakia ones.<sup>[19]</sup> Occasionally, Raman bands of  $\alpha$ -trydimite,  $\alpha$ -cristobalite and quartz can be observed in Raman spectra from opals. In the next paragraphs the Raman spectra of the investigated opals are reported and commented.

All samples from Brazil, Ethiopia, Honduras and Mexico show a very similar Raman spectrum, characterized by a broad band centered at  $\sim 335\text{ cm}^{-1}$  (Fig. 2a). This feature is typical of opal-CT, thus

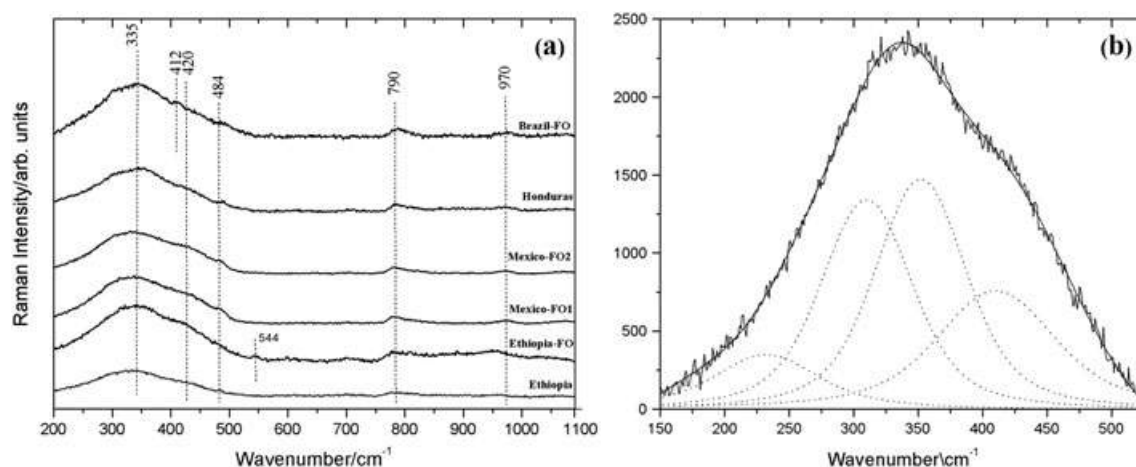


**Figure 2.** Raman spectra of opals a) from Brazil, Honduras, Mexico and Ethiopia. All the spectra have been stacked for a better visualization. b) Non-linear curve fitting of Raman spectrum of sample Ethiopia-FO.

suggesting, according to literature,<sup>[18]</sup> a volcanic origin for these samples. This broad band shows a complex structure with some peaks of weak and medium intensity. In all investigated samples, a band at  $420\text{ cm}^{-1}$  characteristic of  $\alpha$ -trydimite and a band at  $484\text{ cm}^{-1}$  (vibration of Si—O—Si rings with three to four terms) are present. In order to better identify the different contributes in this large band, a deconvolution of the Raman spectrum of Ethiopia-FO sample, in the range  $150\text{--}525\text{ cm}^{-1}$ , is presented in Fig. 2b.<sup>[34]</sup> The band at  $790\text{ cm}^{-1}$  present in all spectra can be assigned to the symmetric Si—O—Si stretching vibration, while the  $970\text{ cm}^{-1}$  band is ascribed to the presence of silanol groups (Si—OH). Only the Raman spectrum of Brazil opal shows a band at  $412\text{ cm}^{-1}$  assigned to the presence of  $\alpha$ -cristobalite domains. In Ethiopia-FO, a not assigned band at  $544\text{ cm}^{-1}$  is also observed.

According to the literature,<sup>[18]</sup> these results suggest a volcanic origin of this group of opals. This is expected for Ethiopia, Honduras and Mexico samples, but not for that from Brazil. Brazil opals are known to have a sedimentary and not a volcanic origin. On the other hand the Brazilian sample analyzed here is a fire opal just like the other three opals from Ethiopia and Mexico (Ethiopia-FO, Mexico-FO1 and Mexico-FO2). This

may explain the apparent contradiction. Despite the different provenance, in fact, the structure of fire opals from many localities around the world has been found to be similar, because the formation of these rare gems occurs at high temperatures.<sup>[37,38]</sup>

In this respect, the classification reported by Rondeau *et al.*,<sup>[19]</sup> based on the temperature formation and not on the mechanism

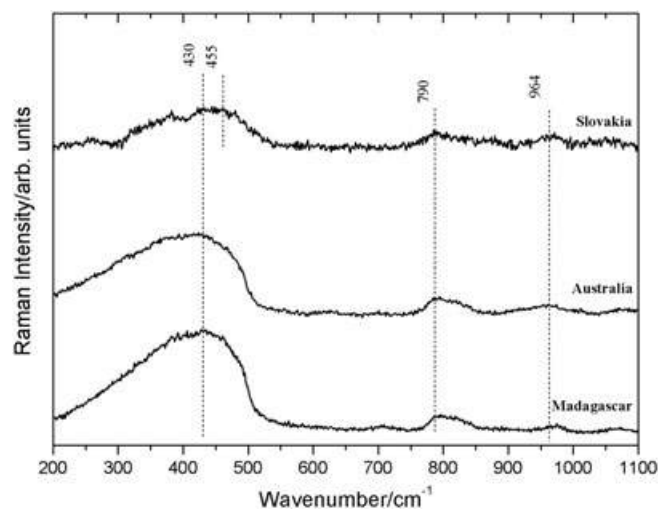


**Figure 3.** Raman spectra of opals from Slovakia, Australia and Madagascar. All the spectra have been stacked for a better visualization.

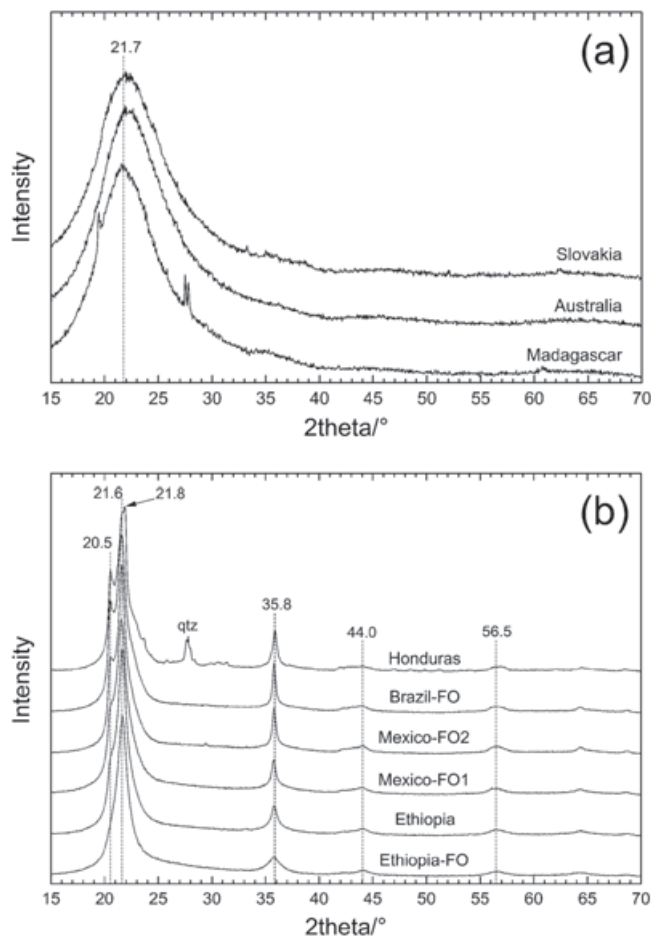


**Figure 4.** XRD patterns of the investigated opals. a) opals-A; b) opals-CT. In b), the label 'qtz' represent quartz.

of formation (sedimentary or volcanic), seems to be more appropriate to interpret our data. Brazil opal has a sedimentary genesis but the high formation temperature ( $100^{\circ}\text{C} < T < 170^{\circ}\text{C}$ ) has influenced the grade of crystallinity of the material.<sup>[10]</sup>

Slovakia, Australia and Madagascar samples show the Raman spectra displayed in Fig. 3. In these spectra, the broad Si—O—Si bending mode is centered at  $430\text{ cm}^{-1}$  as in amorphous silicates, thus suggesting a sedimentary origin (opal-A). We observe also a series of weaker bands around  $797$ ,  $969$  and  $1065\text{ cm}^{-1}$ , corresponding to Si—O or Si—OH vibrations, as detailed in<sup>[18]</sup> and in.<sup>[39]</sup>

### XRD measurements

The X-ray diffraction patterns of the samples from Australia, Madagascar and Slovakia (Fig. 4a) show only a very broad peak

at about  $21.7^{\circ}$  ( $d=4.1\text{ \AA}$ ), that according to,<sup>[40]</sup> identifies these samples as opals-A. All other samples can be classified as opals-CT, because their X-ray diffraction patterns (Fig. 3b) show five well-resolved peaks at about  $20.5^{\circ}$  ( $d=4.30\text{ \AA}$ ),  $21.6^{\circ}$  ( $d=4.11\text{ \AA}$ ),  $35.8^{\circ}$  ( $d=2.50\text{ \AA}$ ),  $44.0^{\circ}$  ( $d=2.03\text{ \AA}$ ) and  $56.5^{\circ}$  ( $d=1.62\text{ \AA}$ ).<sup>[40]</sup> Moreover, we notice that going from Ethiopia-FO to Honduras (that is from bottom to top of Fig. 4b) the main peaks sharpen indicating an increasing degree of order. In particular, in the X-ray diffraction patterns of the Honduras opal, the most intense peak is made up of two relatively well resolved reflections, one at  $21.6^{\circ}$  ( $d=4.11\text{ \AA}$ ) which is typical of opal-CT and the second at  $21.8^{\circ}$  ( $d=4.06\text{ \AA}$ ) which is observed in opal-C. Moreover, in this sample we can observe a peaks at  $\sim 27.7^{\circ}$  ( $d=3.03\text{ \AA}$ ) because of quartz and some other weak and poorly defined reflections.

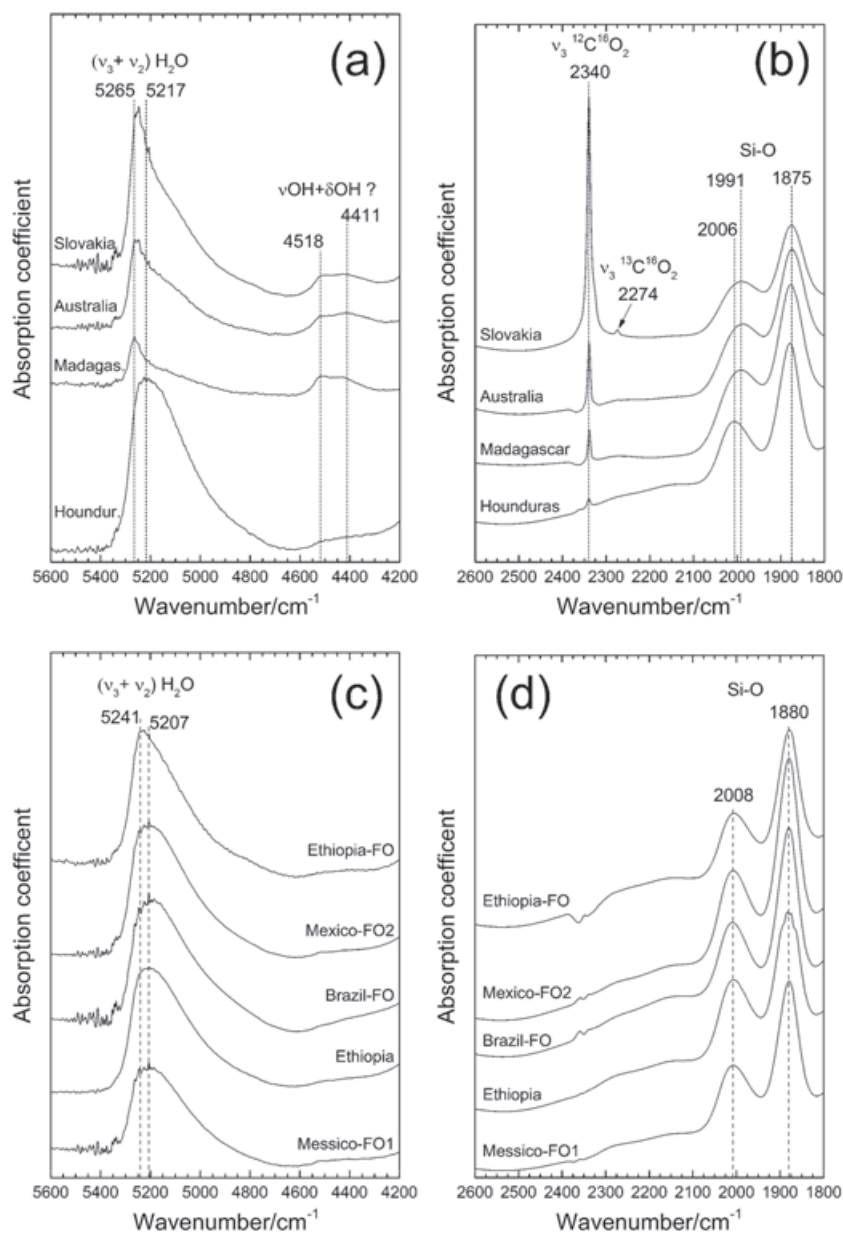


**Figure 5.** Micro-FTIR spectra of the CO<sub>2</sub>-bearing opals in the a) H<sub>2</sub>O/OH combinations and b) CO<sub>2</sub> and Si—O regions. Micro-FTIR spectra of the CO<sub>2</sub>-free opals in the c) H<sub>2</sub>O combinations and d) CO<sub>2</sub> and Si—O regions. All the spectra have been stacked for a better visualization. The regions below  $1800\text{ cm}^{-1}$  and from  $2600$  to  $4200\text{ cm}^{-1}$  are not shown because they are out of range because of the very high absorption.

## FT-IR measurements

### • Powder FTIR spectroscopy

We report FTIR powder spectra, collected in the range 400–4000  $\text{cm}^{-1}$ , in Fig. S5. They are absolutely compatible with those already available in the literature for similar samples.<sup>[41]</sup> In the low frequency region from 400 to 2000  $\text{cm}^{-1}$ , there are three bands centered at 474, 789 and 1100  $\text{cm}^{-1}$  because of the absorptions of the silicate framework vibrations.<sup>[41]</sup> It should be noted that these bands are actually composed of several components, which cannot be adequately resolved (e.g. shoulders at about 500, 940, 1230  $\text{cm}^{-1}$ ). Moreover, in our opals-A (Australia, Madagascar and Slovakia), a band centered at about 796  $\text{cm}^{-1}$ , typical of this type of opals<sup>[42]</sup> is present. At 1643  $\text{cm}^{-1}$  there is a very weak band because of the absorption of the  $\nu_2$  bending vibrations of water ( $\text{H}_2\text{O}$ ). Finally, from 3000 to 3700  $\text{cm}^{-1}$ , there is a very broad multi-component band centered at about 3483  $\text{cm}^{-1}$  and 3650  $\text{cm}^{-1}$  because of the  $\nu_1$  and  $\nu_3$  stretching modes (symmetric and anti-symmetric, respectively) and  $2\nu_2$  combination mode of water ( $\text{H}_2\text{O}$ ) and the stretching vibrations of the O—H groups. In some samples, superimposed on this absorption, there are also a few small components at 3693 and 3620  $\text{cm}^{-1}$  (Slovakia), 3646  $\text{cm}^{-1}$  (Australia) and 3569  $\text{cm}^{-1}$  (Madagascar). Following the work of Ostrooumov<sup>[42]</sup> and references therein, these bands can be attributed to isolated or hydrogen-bonded SiO—H related species.

### • Micro-FTIR spectroscopy and FTIR-FPA imaging.

As shown by Della Ventura *et al.*,<sup>[43]</sup> micro-FTIR spectroscopy represents an extremely powerful and fast tool for studying the presence, speciation and distribution of water and carbon dioxide in glasses and minerals.

On the base of the micro-FTIR spectra (Fig. 5), the studied samples can be divided in two groups, distinguished by the presence or absence of  $\text{CO}_2$ :

- the  $\text{CO}_2$ -bearing opals (Australia, Honduras, Madagascar and Slovakia)
- the  $\text{CO}_2$ -free opals (Brazil-FO, Ethiopia, Ethiopia-FO, Mexico-FO1 and Mexico-FO2).

The micro-FTIR spectra from 1800 to 2600  $\text{cm}^{-1}$  of the  $\text{CO}_2$ -bearing opals (Fig. 5b) show at 2340  $\text{cm}^{-1}$  a very sharp band because of the absorption of the  $\nu_3$  anti-symmetric stretching mode of  $\text{CO}_2$  molecule.<sup>[44]</sup> In detail the  $\text{CO}_2$  content is very low in the Honduras and Madagascar samples and very high in the Slovakia opal. The low intensity absorption because of the  $^{13}\text{CO}_2$   $\nu_3$  anti-symmetric stretching mode<sup>[44]</sup> is also visible in the latter sample. Finally, at about 2006 and 1875  $\text{cm}^{-1}$  there are two broad bands ascribable to the absorptions of the silicate framework vibrations.<sup>[45]</sup>

The micro-FTIR spectra in the same region for the  $\text{CO}_2$ -free opals (Fig. 5d) show only the two broad bands at 2008 and 1880  $\text{cm}^{-1}$ .

The micro-FTIR spectra in the near-infrared (NIR) region, 4200–5600  $\text{cm}^{-1}$ , of the  $\text{CO}_2$ -free opals (Fig. 5c) show a broad ( $\nu_3 + \nu_2$ ) combination mode of  $\text{H}_2\text{O}$  absorption at 5217  $\text{cm}^{-1}$  and very low absorption at lower wavenumbers, where the contribution of the OH groups combination modes is expected. The NIR spectrum of the Honduras opal (Fig. 5a) is very similar, as expected on the basis of its crystallinity degree (opal-CT), although it contains a small amount of  $\text{CO}_2$ .

As far as the other  $\text{CO}_2$ -bearing opals is concerned (Fig. 5a), their NIR spectra are characterized by a broad and asymmetric absorption centered at about 5265  $\text{cm}^{-1}$ , because of the ( $\nu_3 + \nu_2$ ) combination mode of  $\text{H}_2\text{O}$ . There is also a broad and weak absorption, peaked at 4518 and 4411  $\text{cm}^{-1}$  assigned to the OH groups combination modes.<sup>[45]</sup>

The different position and shape of the combination ( $\nu_3 + \nu_2$ )  $\text{H}_2\text{O}$  band indicate strongly different vibrational dynamics of water molecules in  $\text{CO}_2$ -bearing opals with respect to the  $\text{CO}_2$ -free ones.

This is a signature of the different structural arrangement of the hydrogen bonds between water molecules and between water

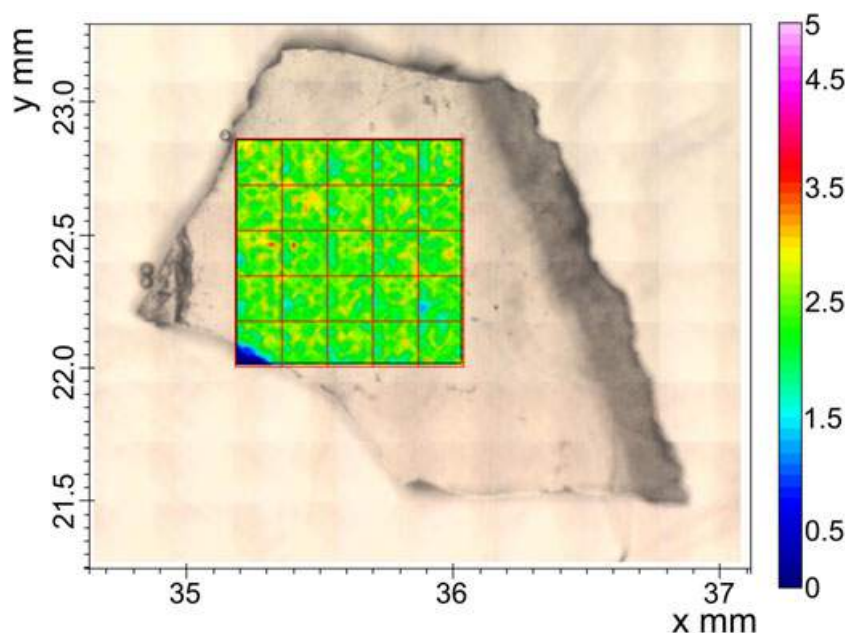


**Figure 6.** FPA micro-FTIR image of the  $\text{CO}_2$  distribution in the Madagascar opal superimposed on the optical image of the sample and the FPA grid (red lines). The FPA image is obtained by integrating the absorbance in the 2350–2330  $\text{cm}^{-1}$  range.

molecules and the opal substrate. Interestingly this is clearly correlated with the occurrence of carbon dioxide and with the degree of crystallinity of opals.

Micro-FTIR imaging shows that the distribution of CO<sub>2</sub> in all the CO<sub>2</sub> bearing opals is quite homogeneous. As an example in Fig. 6 we report the FPA micro-FTIR image of the CO<sub>2</sub> distribution in the sample from Madagascar, obtained by mapping the integrated intensity of the CO<sub>2</sub> band at 2340 cm<sup>-1</sup> in the frame reported.

## Conclusions

Opals are formed by precipitation of aqueous solution, followed by a possible annealing process, either thermally or pressure induced. Hence, initially opal is precipitated in the Opal-A form and then is annealed into the other forms with time. Aim of this study is the investigation of nine natural opals (four of these are fire opals) from Australia, Brazil, Ethiopia, Honduras, Madagascar, Mexico and Slovakia. Raman, FT-IR spectroscopy and X-ray powder diffraction were used to characterize the samples in order to correlate information on gem genesis, geological occurrence and geographical provenance. In fact, in each investigated country, there are at least two or more 'official' mines and often not official ones, with different geological occurrence, influencing the opal genesis. This information could help to avoid frauds and to reconstruct ancient and modern trade routes of gems.

Raman investigations showed that our opals from Brazil, Ethiopia, Honduras and Mexico can be classified as Opal-CT, generally associated to a volcanic genesis. This confirms the known information about the geological occurrence of the mines, with the exception of the Brazil sample. In fact, in literature Brazil opals are reported as sedimentary. This can be explained by considering that the investigated opal from Brazil is a fire opal, generated through a high temperature stage that influenced the crystallinity of the material. Differently, opals from Australia, Slovakia and Madagascar show the typical features of Opal-A, associated to a sedimentary genesis.

XRD analyses confirmed the division into the two categories of opal-A and opal-CT revealed by Raman investigations and added information on long-range order by evidencing a highest degree of crystallinity for Honduras opal with respect to the others.

Powder FT-IR spectroscopy data are compatible with those reported in previous the literature.<sup>[41]</sup> In order to obtain unambiguous information on the presence in opals of CO<sub>2</sub> and H<sub>2</sub>O, it was necessary to perform micro FT-IR. This has demonstrated that all the Opal-A and the Honduras sample contain CO<sub>2</sub>, homogeneously distributed within the gem, while all the other Opal-CT do not.

The concentration of CO<sub>2</sub> is correlated with the line-shape and the maximum position of water combination band at about 5200 cm<sup>-1</sup>. As a matter of fact, CO<sub>2</sub> bearing samples show a band more asymmetric at shifted at higher wavenumbers compared to non CO<sub>2</sub> bearing ones. This suggests that a high content of CO<sub>2</sub> strongly distorts the hydrogen bond network of water trapped in the opal structure, thus influencing the stretching and bending water vibrations. Moreover, the different shape of water bands could be because of the different crystallinity of the investigated samples.

The Honduras sample is the only Opal-CT gem that contains CO<sub>2</sub>, although in smaller concentration with respect to the others. This observation together with its high crystallinity degree suggests that its annealing process is not complete.

This work suggests that the structural and spectroscopic properties of opals strongly depend on the crystallinity degree and CO<sub>2</sub> content and that a multi-techniques approach is mandatory to fully

characterize this kind of materials. Interestingly the CO<sub>2</sub> content is correlated with the vibrational dynamics of water molecules. The observation of the existence of samples with intermediate characteristics between two classes of opals, as for instance the Brazil and Honduras samples investigated here, confirms the need for a rich database of the properties of much more opals coming from different mines.

## References

- [1] R. Webster, *Gems: Their Sources, Description and Identification*, Archon Books, Hamden, CT, **1975**.
- [2] F. Leechman, *The Opal Book*, Lansdowne Press, Sydney, **1984**.
- [3] F. Caucia, C. Ghisoli, L. Marinoni, V. Bordoni, *J. Min. Geochem.* **2012**, *190/1*, 1.
- [4] J. V. Sanders, *Nature* **1964**, *204*(4964), 1151.
- [5] J. V. Sanders, M. J. Murray, *Nature* **1978**, *275*, 201.
- [6] P. J. Darragh, A. J. Gaskin, B. C. Terrell, J. V. Sanders, *Nature* **1966**, *209*(5018), 13.
- [7] J. V. Sanders, *Acta Crystallogr. A* **1968**, *24*(4), 427.
- [8] J. V. Sanders, P. J. Darragh, *Mineral. Rec.* **1971**, *2*(6), 261.
- [9] E. Fritsch, B. Rondeau, M. Ostroumov, B. Lasnier, A. M. Marie, A. Barreau, J. Wery, J. Connoué, S. Lefrant, *Revue de Gemmologie* **1999**, *138/139*, 34–40.
- [10] E. Fritsch, E. Gaillou, M. Ostroumov, B. Rondeau, B. Devouard, A. Barreau, *Eur. J. Mineral.* **2004**, *16*, 743.
- [11] G. D. Mc Orist, A. Smallwood, *J. Radioanal. Nucl. Chem.* **1997**, *223*, 9.
- [12] E. Gaillou, A. Delaunay, B. Rondeau, M. Bouhnik Le Coz, E. Fritsch, G. Cornen, C. Monnier, *Ore Geol. Rev.* **2008**, *34*, 127.
- [13] F. Caucia, C. Ghisoli, I. Adamo, *Neu. Jb Mineral. Abh.* **2009**, *185*, 289.
- [14] F. Caucia, L. Marinoni, V. Bordoni, C. Ghisoli, I. Adamo, *Period. Mineral.* **2012**, *81*, 93.
- [15] M. Simoni, F. Caucia, I. Adamo, P. Galinetto, *Gems Gemol.* **2010**, *46*(2), 114.
- [16] J. B. Jones, E. R. Segnit, *J. Geol. Soc. Aust.* **1971**, *18*(N1), 57.
- [17] A. G. Smallwood, P. S. Thomas, A. S. Ray, *Spectrochim. Acta Part A* **1997**, *53*, 2341.
- [18] M. Ostroumov, E. Fritsch, B. Lasnier, S. Lefrant, *Eur. Mineral.* **1999**, *11*, 899.
- [19] B. Rondeau, E. Fritsch, M. Guiraud, C. Renac, *Eur. J. Mineral.* **2004**, *16*(5), 789.
- [20] P. Bayliss, P. A. Males, *Mineral. Mag.* **1965**, *28*, 429.
- [21] L. C. Barnes, I. J. Townsend, R. S. Robertson, D. C. Scott, *Opal South Australia's Gemstone. Series: Handbook Number 5*, Department of Mines and Energy, Geological Survey of South Australia, Adelaide, **1992** p. 176.
- [22] M. Kastner, J. B. Keene, J. M. Gieskes, *Geochim. Cosmochim. Acta* **1977**, *41*, 1041.
- [23] J. H. F. Jansen, S. J. Van der Gaast, *Mar. Geol.* **1988**, *83*, 1.
- [24] H. Graetsch, *Rev. Mineral.* **1994**, *29*, 209.
- [25] T. Nagase, M. Akizuki, *Can. Mineral.* **1997**, *35*, 947.
- [26] F. Elsass, D. Dubroeuq, M. Thiry, *Clay Minerals* **2000**, *35*, 477.
- [27] H. Graetsch, in *Silica: Physical Behavior, Geochemistry, and Materials Applications*, (Eds: J. Heaney, C. T. Prewitt, G. V. Gibbs), Chantilly, Virginia, **1994**, pp. 209–232.
- [28] M. Liesegang, R. Milke, *Am. Mineral.* **2014**, *99*, 1488.
- [29] P. Bayliss, P. A. Males, *Mineral. Mag.* **1965**, *35*, 429.
- [30] R. J. Spencer, A. A. Levinson, J. I. Koivula, *Gems Gemol.* **1992**, *28*, 28.
- [31] J. B. Jones, J. V. Sanders, E. R. Segnit, *Nature* **1964**, *204*, 990.
- [32] G. Giuliani, M. Chaussidon, H.-J. Schubnel, D. Piat, C. Rollion-Bard, C. France-Lanord, D. Giard, D. De Narvaez, B. Rondeau, *Science* **2000**, *287*, 631.
- [33] K. A. Rodgers, W. A. Hampton, *Mineral. Mag.* **2003**, *67*, 1.
- [34] A. Ilieva, B. Mihailova, Z. Tsintsov, O. Petrov, *Am. Mineral.* **2007**, *92*, 1325.
- [35] G. Della Ventura, F. Bellatreccia, A. Marcelli, M. Cestelli Guidi, M. Piccinini, A. Cavallo, M. Piochi, *Anal. Bioanal. Chem.* **2010**, *397*, 2039.
- [36] A. G. Smallwood, *Aust. Gemmol.* **2000**, *20*(9), 363.
- [37] E. Fritsch, E. Gaillou, B. Rondeau, A. Barreau, *J. Non Cryst. Solids* **2006**, *352*, 3957.
- [38] E. Fritsch, *Eur. J. Mineral.* **2004**, *16*, 789.
- [39] D. P. Zarubin, *J. Non-Cryst. Solids* **2001**, *286*, 80.

- [40] C. Ghisoli, F. Caucia, L. Marinoni, *Powder Diffr.* **2010**, *25*, 274.  
[41] I. Adamo, C. Ghisoli, F. Caucia, *Neu. Jb. Mineral. Abh.* **2010**, *187*(1), 63.  
[42] M. Ostrooumov, *Spectrochim. Acta A* **2007**, *68*, 1070.  
[43] G. Della Ventura, A. Marcelli, F. Bellatreccia, *Rev. Mineral. Geochem.* **2014**, *78*, 447.  
[44] V. M. Khomeenko, K. Langer, *Am. Mineral.* **2005**, *90*, 1913.  
[45] S. Newman, E. M. Stolper, S. Epstein, *Am. Mineral.* **1986**, *71*, 1527.

## Supporting information

Additional supporting information may be found in the online version of this article at the publisher's web site.